PROCEEDINGS OF SPIE

SPIEDigitalLibrary.org/conference-proceedings-of-spie

Multi-energy spectral photon-counting CT in crystal-related arthropathies: initial experience and diagnostic performance in vitro

Anais Viry, Aamir Y. Raja, Tracy E. Kirkbride, Chloe Choi, Lisa K. Stamp, et al.

Anais Viry, Aamir Y. Raja, Tracy E. Kirkbride, Chloe Choi, Lisa K. Stamp, Nicola Dalbeth, Christele Combes, Francis R. Verdun, Nigel G. Anderson, Fabio Becce, "Multi-energy spectral photon-counting CT in crystal-related arthropathies: initial experience and diagnostic performance in vitro," Proc. SPIE 10573, Medical Imaging 2018: Physics of Medical Imaging, 1057351 (9 March 2018); doi: 10.1117/12.2293458

SPIE.

Event: SPIE Medical Imaging, 2018, Houston, Texas, United States

Multi-energy spectral photon-counting CT in crystal-related arthropathies: Initial experience and diagnostic performance in vitro

Anais Viry[a], Aamir Y. Raja[b], Tracy E. Kirkbride[c], Chloe Choi[d], Lisa K. Stamp[e], Nicola Dalbeth[d], Christele Combes[f], Francis R. Verdun[a], Nigel G. Anderson[d], Fabio Becce[g]

[a]Institute of Radiation Physics, Lausanne University Hospital, Lausanne, Switzerland
[b]Department of Radiology, University of Otago, Christchurch, New Zealand
[c]Ara Institute of Canterbury, Christchurch, New Zealand
[d]Department of Medicine, University of Auckland, Auckland, New Zealand
[e]Department of Medicine, University of Otago, Christchurch, New Zealand
[f]CIRIMAT, Université de Toulouse, CNRS, INPT, UPS, ENSIACET, Toulouse, France
[g]Department of Diagnostic and Interventional Radiology, Lausanne University Hospital, Lausanne, Switzerland

ABSTRACT

Purpose: We aimed to determine the in-vitro diagnostic performance of multi-energy spectral photon-counting CT (SPCCT) in crystal-related arthropathies.

Methods: Four crystal types (monosodium urate, MSU; calcium pyrophosphate, CPP; octacalcium phosphate, OCP; and calcium hydroxyapatite, CHA) were synthesized and blended with agar at the following concentrations: 240, 88, 46, and 72 mg/mL, respectively. Crystal suspensions were scanned on a pre-clinical SPCCT system at 80 kVp using the following four energy thresholds: 20, 30, 40, and 50 keV. Differences in linear attenuation coefficients between the various crystal suspensions were compared using the receiver operating characteristic (ROC) paradigm. Areas under the ROC curves (AUC), sensitivities, specificities, and diagnostic accuracies were calculated. Crystal differentiation was considered successful if AUC>0.95.

Results: For each paired comparison of crystal suspensions, AUCs were significantly higher in the first energy range (20-30 keV). In the first energy range, MSU was confidently differentiated from CPP (sensitivity, 0.978; specificity, 0.990; accuracy, 0.984) and CHA (sensitivity, 0.957; specificity, 0.970; accuracy, 0.964), while only moderately distinguished from OCP (sensitivity, 0.663; specificity, 0.714; accuracy, 0.688). CPP was confidently differentiated from OCP (sensitivity, 0.950; specificity, 0.954; accuracy, 0.952), while only moderately from CHA (sensitivity, 0.564; specificity, 0.885; accuracy, 0.727). OCP was accurately differentiated from CHA (sensitivity, 0.898; specificity, 0.917; accuracy, 0.907).

Conclusions: Multi-energy SPCCT can accurately differentiate MSU from CPP and CHA, CPP from OCP, and OCP from CHA in vitro. The distinction between MSU and OCP, and CPP and CHA is more challenging.

Keywords: Photon-counting imaging, multi-energy spectral CT, crystal-related arthropathies, monosodium urate, calcium pyrophosphate, calcium hydroxyapatite.

1. INTRODUCTION

Crystal-related arthropathies are a growing global health problem and imaging plays an important role in the diagnosis [1] [2]. Indeed, distinguishing crystal type, whether monosodium urate or one of the calcium crystal types is a clinical challenge because diagnosis and treatment depends on the crystal type involved. Although clinical imaging has made

Medical Imaging 2018: Physics of Medical Imaging, edited by Joseph Y. Lo, Taly Gilat Schmidt, Guang-Hong Chen, Proc. of SPIE Vol. 10573, 1057351
 · doi: 10.1117/12.2293458

substantial progress in recent years, particularly with the development of dual-energy CT (DECT) protocols in people with longstanding and/or tophaceous gout[3], the diagnostic performance of DECT remains limited in the early stages of gout[4]. Moreover, while DECT is relatively accurate in distinguishing monosodium urate (MSU) from the various calcium deposits, there is currently no imaging technique capable of noninvasively differentiating one calcium crystal type from another in crystal-related arthropathies, whether in or around the joints.

Multi-energy spectral photon counting CT can measure different energy ranges, up to eight energy bins for each pixel for the Medipix chip[5]. Distinguishing MSU from calcium crystals is no longer a challenge especially for lower energy ranges. We hypothesized that the multiple energy capability of spectral photon-counting CT (SPCCT) could not only distinguish MSU from calcium crystals, but also distinguish between calcium crystal types. Therefore, we aimed to determine the in-vitro diagnostic performance of SPCCT to discriminate crystal type in crystal-related arthropathies using a task-based methodology.

2. MATERIALS AND METHODS

2.1 Preparation of crystal samples

Four suspensions of calcium hydroxyapatite (CHA) at 72 mg/mL, octacalcium phosphate (OCP) at 46 mg/mL, calcium pyrophosphate (CPP) at 88 mg/mL, and monosodium urate (MSU) at 240 mg/mL were prepared by blending synthetic crystal powders with agar. These concentrations were selected based on those found on clinical DECT images of patients affected by the various crystal-related arthropathies. A liquid agar solution at 1.5% was prepared by diluting agar powder in water at 100°C. For each suspension, the exact amount of crystal was weighed and poured into vials containing 1 mL of liquid agar. The mixture was then poured into 200 µL Eppendorf vials. Agar was chosen as the medium for preparation of calcium crystal samples because the quick solidification of agar can ensure that crystal suspensions are evenly dispersed in the volume of the vial. In addition, the linear attenuation coefficient of agar is close to soft tissue and will thus not interfere with calcium attenuation. Table 1 reports the effective Z numbers (Z_{eff}) and density of each crystal involved in this study.

Table 1. Effective Z numbers and density of each crystal.

	Z_{eff}	Density
Monosodium urate (MSU)	9.51	2.12 g/cm^3
Calcium pyrophosphate (CPP)	14.58	2.56 g/cm^3
Octacalcium phosphate (OCP)	15.05	2.67 g/cm^3
Calcium hydroxyapatite (CHA)	15.86	3.16 g/cm^3

2.2 Phantom

A customized 25-mm-diameter cylindrical polymethylmethacrylate (PMMA) phantom containing twelve 6-mm-diameter holes was used. 200 µL. Four Eppendorf vials containing MSU and the three different calcium crystal suspensions were inserted into the holes. A vial containing only agar was also added to serve as a reference.

2.3 Acquisition parameters

The customized PMMA phantom containing the various crystal suspensions was scanned on a pre-clinical multi-energy SPCCT system (MARS Bioimaging Ltd, Christchurch, New Zealand). Tube voltage was set to 80 kVp with a 2 mm additional aluminum filtration while tube current and exposure time were fixed to 27 µA and 220 ms, respectively, to give detector count rates of less than 5 per millisecond. Image acquisition was done using 720 circular projections over 360°.

The detector chip Medipix3RX is an energy-resolving single photon-counting detector that enables spectral x-ray imaging by counting and measuring the energy of individual photons transmitted through an object and assigning them to user-defined energy bins[6 5]. In this study, four energy thresholds of 20, 30, 40, and 50 keV were used. The slice thickness and field of view were equal to 0.1 mm and 48 x 48mm with 480 pixels, yielding cubic voxels of 0.1 x 0.1 x

0.1 mm^3. Images were reconstructed for each energy range using proprietary MARS Simultaneous Algebraic Reconstruction Technique (SART).

2.4 Image Analysis

Images in which pixels are expressed in linear attenuation coefficients were directly analyzed to assess the potential discrimination between the various crystal combinations. No material decomposition algorithm was applied in this study. The first step was to subtract the mean linear attenuation value of the agar-only vial to linear attenuation values from that of each of the various crystal suspensions, for each energy bin. Then, for each vial, fifteen consecutive circular regions of interest of 8 mm^2 were sampled along the volume, and pixel data extracted. Histograms of linear attenuation coefficients were then plotted for each energy bin and for each crystal suspension. In order to assess the discrimination between pixel values for a pair of samples, a receiver operating characteristic curve (ROC) curve was plotted. The area under the ROC curve (AUC) was computed and used as the figure of merit to assess the differentiation between two crystals considering that the higher the AUC value, the easier would be the discrimination task. The energy range that allowed optimal discrimination for each crystal combination was determined. For this energy range, on the ROC curve the cut-off that maximized the sum between sensitivity and specificity was determined in order to calculate sensitivity, specificity, accuracy, positive predictive value (PPV) and negative predictive value (NPV). The discrimination between any two crystal suspensions was considered successful if AUC > 95%. For each quantitative result, 95% CI was calculated using a bootstrap method (with resampling) using 1000 iterations.

3. RESULTS

3.1 Histograms

Figure 1 shows the overlap of histograms of linear attenuation coefficients between MSU, OCP, CPP and CHA for each of the four energy bins. Table 1 summarizes the mean attenuation values and the standard deviation for each crystal as a function of the energy threshold. As expected, mean linear attenuation values decreased for the higher energy ranges.

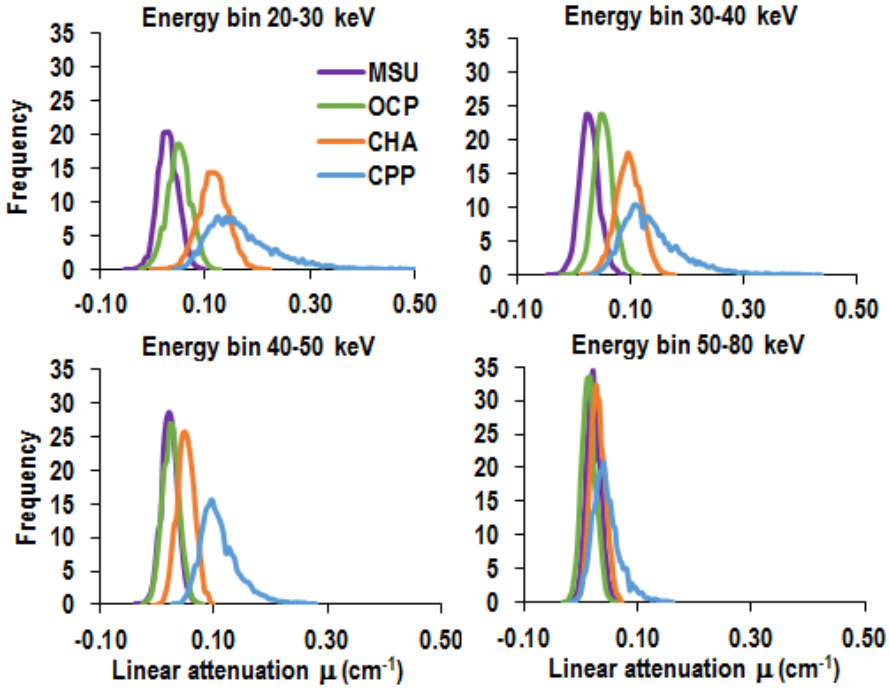

Figure 1. Histograms of linear attenuation coefficients of CHA, OCP, CPP and MSU crystals for the four energy bins

Table 2. Mean linear attenuation values and standard deviation of the four crystals for each of the four energy bins

	Energy bin 20-30 keV	Energy bin 30-40 keV	Energy bin 40-50 keV	Energy bin 50-80 keV
MSU	0.033 +/- 0.019	0.031 +/- 0.017	0.025 +/- 0.017	0.023 +/- 0.012
OCP	0.052 +/- 0.022	0.048+/- 0.019	0.027 +/- 0.015	0.015 +/- 0.012
CPP	0.175 +/- 0.07	0.142 +/- 0.05	0.075 +/- 0.034	0.046 +/- 0.024
CHA	0.118 +/- 0.028	0.099 +/- 0.022	0.053 +/- 0.015	0.32 - 0.013

3.2 ROC Curves

ROC curves differentiating pairs of crystal suspensions (pairwise comparisons) were plotted for the three combinations between MSU and each calcium crystal sample (MSU vs CPP, MSU vs OCP, and MSU vs HA); see figure 2, and for three pairs of calcium crystal combinations (OCP vs HA, OCP vs CPP, HA vs CPP); see figure 3. For each material combination, AUC result is plotted as a function of the energy bins in figure 4. Instead, AUC values decrease for the higher energy bins; the discrimination between crystal compositions becomes then more difficult at higher energy bins. For all pairs of crystal combination, the AUC value is maximum for the lowest energy range (20- 30 keV).

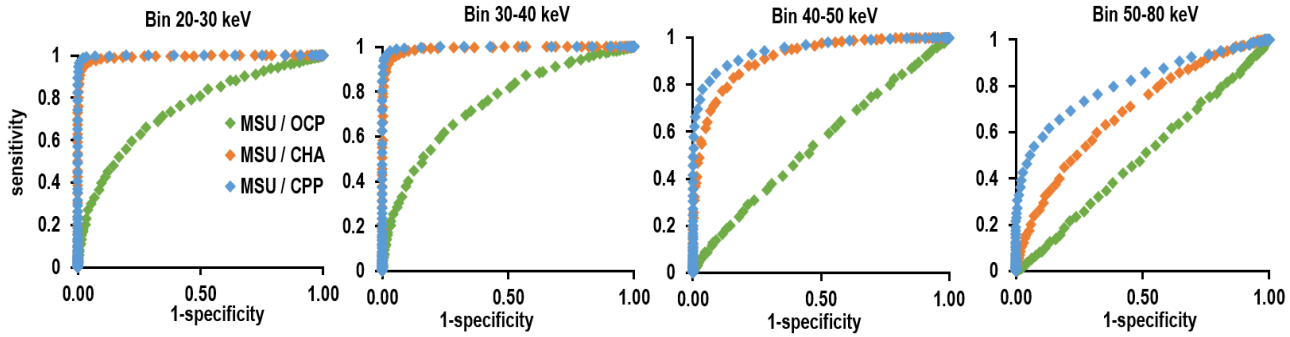

Figure 2. ROC curves for the three combinations between MSU and the various calcium crystals.

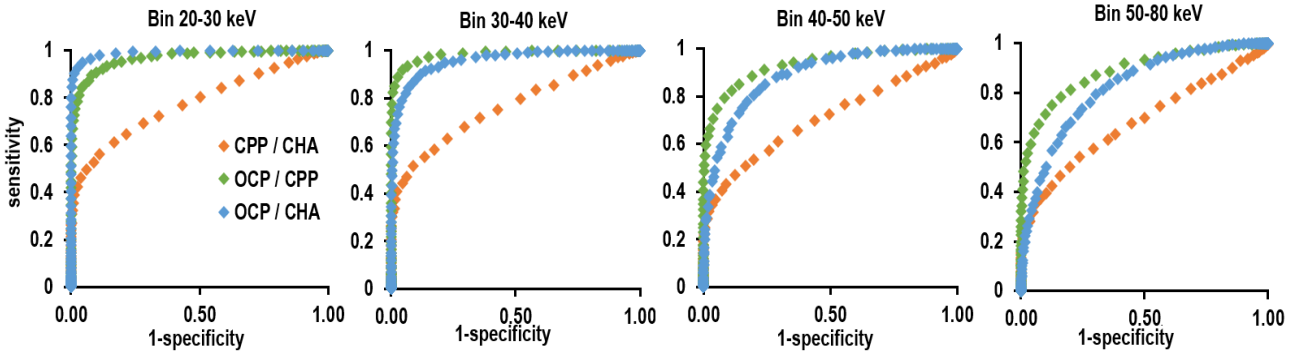

Figure3. ROC curves for the three combinations with calcium crystals.

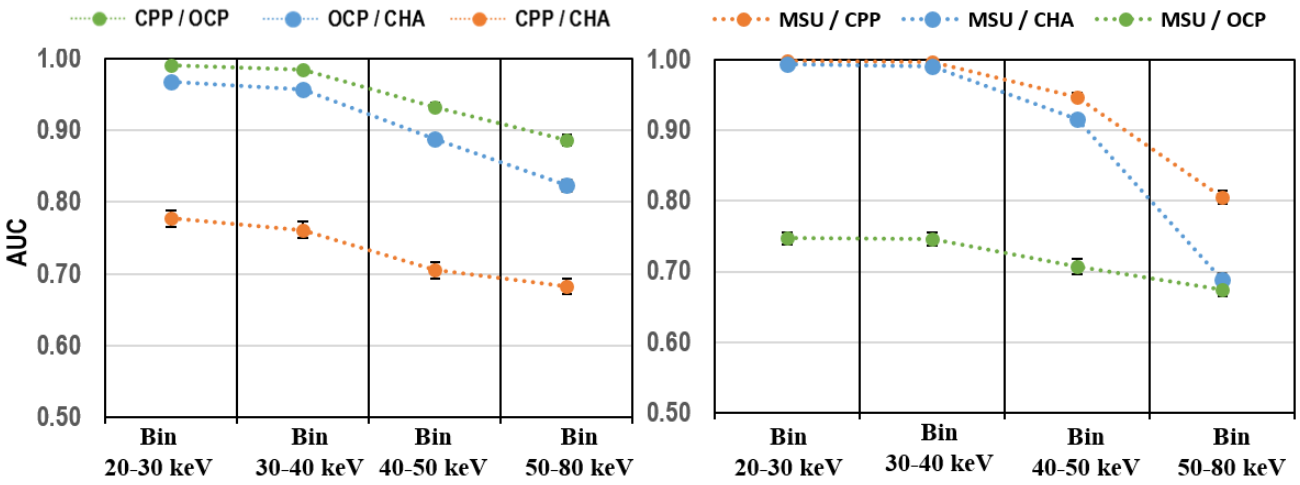

Figure 4. AUC results as a function of energy bins for all crystal combinations. Error bars represent the 95% CI.

3.3 Diagnostic performances

In Table 3, AUC and best parameter performances, sensibility, specificity accuracy, positive predictive value (PPV) and negative predictive value (NPV) for each crystal combination are summarized for the 20-30 keV energy range.

Table 3: Mean values for AUC and best parameter performances for each crystal combination investigated. 95% confidence intervals were detailed in brackets. The AUC values >95% are in bold. 95% CI were indicated in brackets.

	AUC	Sensitivity	Specificity	Accuracy	PPV	NPV
MSU vs CPP	**0.999** [0.998-1.000]	0.986 [0.974-0.998]	0.988 [0.974-1]	0.987 [0.980-0.994]	0.988 [0.975-1.000]	0.986 [0.974-0.998]
MSU vs OCP	0.747 [0.739-0.756]	0.698 [0.620-0.776]	0.714 [0.631-0.797]	0.706 [0.686-0.726]	0.711 [0.668-0.753]	0.704 [0.667-0.740]
MSU vs CHA	**0.994** [0.992-0.995]	0.966 [0.948-0.985]	0.973 [0.952-0.993]	0.970 [0.960-0.979]	0.973 [0.953-0.993]	0.967 [0.949-0.985]
CPP vs OCP	**0.991** [0.989-0.993]	0.950 [0.925-0.976]	0.963 [0.933-0.992]	0.957 [0.945-0.968]	0.963 [0.935-0.991]	0.951 [0.928-0.974]
CPP vs CHA	0.777 [0.766-0.789]	0.673 [0.594-0.753]	0.780 [0.673-0.888]	0.758 [0.682-0.833]	0.758 [0.668-0.833]	0.706 [0.666-0.740]
OCP vs CHA	**0.968** [0.964-0.971]	0.912 [0.882-0.962]	0.922 [0.881-0.962]	0.918 [0.903-0.930]	0.922 [0.887-0.956]	0.913 [0.882-0.944]

Comparing the combination between MSU and the three calcium crystals, AUC values showed that MSU can be accurately differentiated from CPP and CHA (AUC > 0.95) but can only be moderately distinguished from OCP (AUC=0.747). The best discrimination performances were found between MSU and CPP, and between MSU and CHA yielding an accuracy of 98.7 % (98.0% - 99.4%) and 97.0% (96.0% - 97.9%), respectively.

Then, comparing each pair of calcium crystals, OCP can be accurately distinguished from CPP and CHA (AUC>0.95) with an accuracy of 95.7 % (94.5% - 96.8%) and 91.8% (90.3% - 93%). However, CPP cannot be reliably discriminated from CHA (AUC=0.777).

4. DISCUSSION

This study shows that multi-energy SPCCT has the potential to discriminate crystals involved in crystal-related arthropathies. Firstly, MSU can be accurately differentiated from CHA and CPP. This result is in line with previous findings using a DECT technique, for people with tophaceous gout[4]. For the discrimination between pairs of calcium crystals, our in vitro study shows that multi-energy SPCCT could also differentiate CPP from OCP, and OCP from CHA. Currently, no other X-ray imaging technique has shown this potential. If this promising result translates into clinical imaging practice, then non-invasive and timely specific diagnosis of crystal-related arthropathies could be achieved, not only for tophaceous gout. A better understanding of the in-vivo physiopathology of these diseases might also be achieved.

Regarding the performance of multi-energy SPCCT for the challenging discrimination task, as expected, the discrimination depends on the selection of the energy threshold: the lower the energy range, the better will be the discrimination. This dependence comes directly from the X-ray attenuation law through the various compounds. The K-edge of calcium is very low (4 keV), so this property cannot be used with DECT or multi-energy SPCCT technique. However, the difference in linear attenuation coefficients between calcium crystals will be higher for low energy photons with a predominant photoelectric effect than for high energy photons. For this study, the imaging protocol chosen was optimized from preliminary testing. The choice of energy threshold and magnitude of energy was made in order to limit the risk of pulse pile-up effect and saturation of the detector. In order to increase the potential of discrimination between the crystals with multi-energy SPCCT, one should try to optimize the tube potential or optimize the selected energy ranges. Based on our previous study, optimization of the energy thresholds has a greater influence on crystal discrimination than optimizing tube potential[7]. The tuning of the energy threshold should focus on lower energy ranges while maintaining a sufficient number of photons to acquire an image with a good image quality level. For crystal arthropathies, usually manifesting in the peripheral joints, the selection of energy ranges from 20 to 80 keV should be clinically usable.

Regarding the methodology, it appears essential for future investigations to find an objective methodology to quantify a discrimination task with multi-energy SPCCT. The ROC paradigm was proposed to assess the discrimination between compounds because the technique is widely used to assess the diagnostic accuracy of medical imaging techniques focusing on the correct classification of two distinct classes[8]. In our case, the two classes corresponds to two different compounds. To our knowledge, it is the first time that this methodology is proposed for spectral imaging data and it could be a promising and simple methodology to develop.

The major strength of this work is the use of a new spectral SPCCT prototype that will be translating to human. Its main limitations are that we studied ex vivo crystal samples, with only one concentration per sample, however the concentrations chosen were related to concentrations that could be found in patients.

5. CONCLUSION

Multi-energy SPCCT can accurately differentiate MSU from CPP and CHA, CPP from OCP, and OCP from CHA in vitro. The distinction between MSU and OCP, and CPP and CHA is more challenging. Further studies will determine whether these promising preliminary results will translate to excised human specimens, and to clinical practice.

REFERENCES

[1] McQueen, F. M., Doyle, A. and Dalbeth, N., "Imaging in the Crystal Arthropathies," Rheum. Dis. Clin. N. Am. **40**(2), 231–249 (2014).

[2] Neogi, T., Jansen, T. L. T. A., Dalbeth, N., Fransen, J., Schumacher, H. R., Berendsen, D., Brown, M., Choi, H., Edwards, N. L., Janssens, H. J. E. M., Lioté, F., Naden, R. P., Nuki, G., Ogdie,

A., Perez-Ruiz, F., Saag, K., Singh, J. A., Sundy, J. S., Tausche, A.-K., et al., "2015 Gout classification criteria: an American College of Rheumatology/European League Against Rheumatism collaborative initiative," Ann. Rheum. Dis. **74**(10), 1789–1798 (2015).
[3] Choi, H. K., Burns, L. C., Shojania, K., Koenig, N., Reid, G., Abufayyah, M., Law, G., Kydd, A. S., Ouellette, H. and Nicolaou, S., "Dual energy CT in gout: a prospective validation study," Ann. Rheum. Dis. **71**(9), 1466–1471 (2012).
[4] Bongartz, T., Glazebrook, K. N., Kavros, S. J., Murthy, N. S., Merry, S. P., Franz, W. B., Michet, C. J., Akkara Veetil, B. M., Davis, J. M., Mason, T. G., Warrington, K. J., Ytterberg, S. R., Matteson, E. L., Crowson, C. S., Leng, S. and McCollough, C. H., "Dual-energy CT for the diagnosis of gout: an accuracy and diagnostic yield study," Ann. Rheum. Dis. **74**(6), 1072–1077 (2015).
[5] Ronaldson, J. P., Zainon, R., Scott, N. J. A., Gieseg, S. P., Butler, A. P., Butler, P. H. and Anderson, N. G., "Toward quantifying the composition of soft tissues by spectral CT with Medipix3: Quantifying the composition of soft tissues," Med. Phys. **39**(11), 6847–6857 (2012).
[6] Ballabriga, R., Alozy, J., Blaj, G., Campbell, M., Fiederle, M., Frojdh, E., Heijne, E. H. M., Llopart, X., Pichotka, M., Procz, S., Tlustos, L. and Wong, W., "The Medipix3RX: a high resolution, zero dead-time pixel detector readout chip allowing spectroscopic imaging," J. Instrum. **8**(02), C02016–C02016 (2013).
[7] Kirkbride, T. E., Raja, A. Y., Müller, K., Bateman, C. J., Becce, F. and Anderson, N. G., "Discrimination Between Calcium Hydroxyapatite and Calcium Oxalate Using Multienergy Spectral Photon-Counting CT," Am. J. Roentgenol. **209**(5), 1088–1092 (2017).
[8] Thompson, J. D., Manning, D. J. and Hogg, P., "Analysing data from observer studies in medical imaging research: An introductory guide to free-response techniques," Radiography **20**(4), 295–299 (2014).